Journal of Optoelectronics and Advanced Materials Vol. 7, No. 3, June 2005, p. 1599 -1604

OPTIMIZATION AND DESIGN OF ACOUSTO-OPTIC TUNABLE FILTERS

Z. Yuanfeng*, Y. Jisheng

Department of Applied Physics, Tianjin University, Tianjin 300072, China

The set of equations describing the acousto-optic diffraction problem and bounding the amplitudes of transmitted and diffracted light and their solution that determined the optical wave amplitudes at the acouto-optic tunable filters output is presented. Based on this feature the acoustic intensity of different transducer geometries is calculated, the sidelobe of AOTF can be reduced by changing the transducer geometry and it is proved by experiments. Furthermore by calculating the acoustic intensity distribution of different transducers, optimum transducer geometry is designed.

(Received February 24, 2005; accepted May 26, 2005)

Keywords: Sidelobe, Acoustic intensity distribution, Transmission function

1. Introduction

Acousto-optic tunable filters (AOTFs) are solid state wavelength tunable optical filters. Modern AOTFs are constructed by attaching piezoelectric transducers to an appropriate crystalline material. By driving the transducers at the appropriate frequency, a series of perturbations traverse the material. Interactions of photons with these perturbations allow the AOTF to selectively diffract a single narrow-bandpass wavelength. The wavelength may be varied by changing the applied frequency. And it can offer broad tuning range, fast tuning speed, non-multi-orders diffraction, and non-moving parts. However there are disadvantages with this apparatus: the side lobes (secondary maxima) are rather large, which is highly undesirable for a spectrometer. This is due to the fact that the sound amplitude field is a block function (constant amplitude inside the crystal, zero outside), and its Fourier transform gives the transfer function, at least in the weak sound amplitude case. Therefore, a steep rise in the amplitude field is translated, by Fourier transform properties, into high side lobes.

To reduce the sidelobes many different approaches have been investigated: cascading of several devices [1,2] and using a weighted coupling technique [3,4], But the approaches of them require more complex devices and they are not directly applicable to switch structures. In this paper another new approach is presented: the sidelobe is suppressed by changing the transducer geometry, and the result is proved by experiments.

2. Deduction of general relation

The typical AO (acousto-optic) cell with an orthogonal geometry of interaction is depicted in Fig. 1. An acoustic beam is generated by the plane piezotransducer. The set of equations describing the AO diffracted problem and bounding the amplitudes of transmitted E_t and diffracted E_d light in this case has the form: [5]

* Corresponding author: yuanfengzhu@126.com

$$\frac{dE_t}{dx} = -\frac{q}{2} E_d(x) \exp(-i\eta x) \tag{1}$$

$$\frac{dE_d}{dx} = \frac{q}{2} E_t(x) \exp(i\eta x) \tag{2}$$

Here q is the coefficient proportional to the Acoustic wave amplitude and $\eta = (k_t + K - k_d) \cdot e_x$ is the mismatch parameter; k_t , k_d and K are the wave vectors of the transmitted and diffracted light and of sound; e_x is the unit vector along the x axis.

The solution of system (1) and (2) at the boundary conditions

$$E_d(0) = 0;\ E_t(0) = E_i \tag{3}$$

is defined by relations

$$E_d(l) = \exp(i\eta l/2) \frac{qE_i}{(q^2+\eta^2)^{1/2}} \sin(q^2+\eta^2)^{1/2} \frac{l}{2} \tag{4}$$

$$E_t(l) = E_i \exp(-i\eta l/2)(\cos(q^2+\eta^2)^{1/2} \frac{l}{2} + \frac{j\eta}{(q^2+\eta^2)^{1/2}} \sin(q^2+\eta^2)^{1/2} \frac{l}{2}) \tag{5}$$

Here E_i is the amplitude of the incident light. The solution (4) and (5) is the amplitude optical waves amplitudes at the AO cell output (when x=l).

The diffracted light intensity at the AO cell output $I_d = E_d(l)E_d^*(l)$ is a function of Raman-Nath parameter ql and the mismatch ηl .The last is defined by an acoustic frequency $f = Kv/2\pi$ and the incident light wavelength $\lambda = 2\pi n_t / k_t$. Here v is the sound velocity, n_t is the refraction index for the incident light. Thus, $P(\eta l) = I_d(\eta l)/I_d(0)$ is the function which describes the AO cell transmission function.

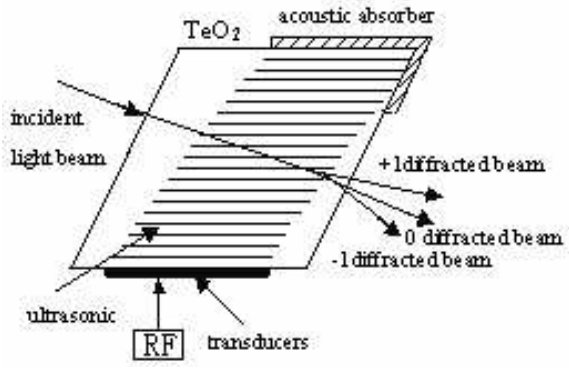

Fig. 1. Schematic diagram of AOTF.

Relation (4) and (5) show that the transmission function depends on the Raman-Nath parameter. Relation (1) and (2) testify that the function $E_d(\eta)$ is the Fourier spectrum of the qE_t product, i.e. of the product of an acoustic field amplitude distribution along the *x* axis and transmitted optical beam amplitude. Thus, for the alteration of the transmission function it is necessary to vary an acoustic field amplitude distribution. And if the coupling coefficient is tapered within the interaction length with a soft onset and cutoff at the beginning and at the end of the structure, then the sidelobes are suppressed. The acoustic intensity is proportional to the AO coupling efficient, So if the acoustic intensity is varied from a minimum at the ends to a maximum in the middle of the interaction region, we can lower the sidelobe [6][7].

3. Calculation of acoustic intensity and the acoustic distributions of different transducers

The acoustic intensity is closely relative to the acoustic pressure, so we discuss acoustic pressure firstly [8].

In Fig. 2 *M* is a random spot on the optical channel, h_0 is the vertical distance from *M* to surface of the transducer, ds (*x*, *z*) is a small area of the transducer, *h* is the distance from *M* to ds (*x*, *z*).

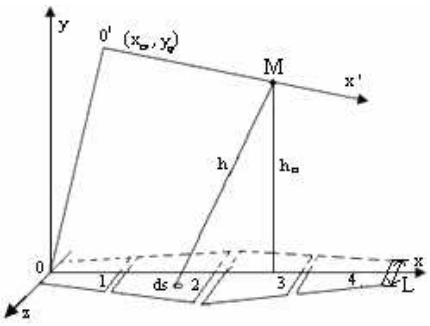

Fig. 2. The chart for calculation of the acoustic intensity.

Based on the formula of acoustic pressure, we can obtain:

$$dp = \mathrm{i}\frac{k\rho v}{2\pi h}u_A ds e^{\mathrm{i}(\omega t - kh)} \tag{6}$$

In this paper, the density, amplitude and frequency can approximately be considered as independent of the coordinate *x* and *z*, with time coefficient neglected. Through calculations, the acoustic pressure should be written by:

$$p \propto \iint_s \frac{e^{-\mathrm{i}kh}}{2\pi h} ds = \int_a^b \frac{e^{-\mathrm{i}kh}}{2\pi h} dx \int_{-z(x)}^{z(x)} dz \tag{7}$$

Because the diffraction efficiency and the bandwidth of a sole transducer are too small, we section the transducer into four sections (1, 2, 3, 4) to improve the bandwidth and the acoustic

conversion efficiency. The sections are connected in series, so the electrodes of 2, 3 are contrary to the electrodes of 1, 4, and the phase is reverse. Provided that P_1 and P_4 are negative, P_2 and P_3 are positive.

So the acoustic pressure on the *M* spot can be written as follows:

$$p_M = -p_1 - p_4 + p_2 + p_3 \tag{8}$$

In the paper, Fresnel approximation is adopted to equation (7) (the meaning of h_0, x, z, x' is shown in Fig. 2. Where h is obtained:

$$h \cong \mathrm{h}_0[1+\frac{(x-\mathrm{x}_0-x'\cos\alpha)^2+\mathrm{z}^2}{2\mathrm{h}_0{}^2}] \tag{9}$$

Because the T_eO_2 crystal is anisotropic, acoustic wave is different in each direction. In *t*-*z*-cut (*t*: [110] *z*: [001]), the equation is written [9]:

$$\frac{k}{\omega}=\left(\frac{\rho}{\frac{c_{11}-c_{12}}{2}\cos^2\theta+c_{44}\sin^2\theta}\right)^{1/2} \tag{10}$$

For the crystal, c_{11} = 5.57, c_{12} = 5.12, c_{44} = 2.65(the unit is 10^{10} N/m^2), and $\theta(\theta=102.9^o-\arcsin(\frac{h_o}{h}))$ is the angle between direction of propagation and [110].

By changing the width of transducer from 6mm to 0, three transducer geometries are designed, as shown in Fig. 3. The acoustic intensity distributions of them are calculated based on the equation $I \propto |P|^2$, and their acoustic intensity distribution charts are shown in Fig. 4.

From Fig. 4, we know the transducer with L = 0 mm is better in sidelobe suppression.

(a) L = 6 mm (b) L = 3 mm (c) L = 0 mm

Fig. 3. Transducers with different width.

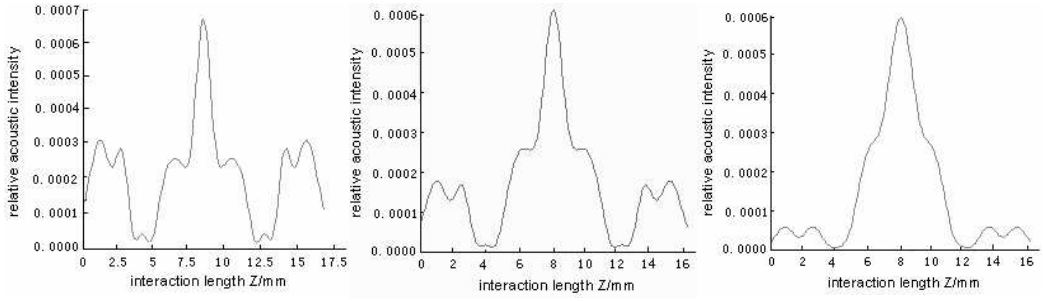

(a) L = 6 mm (b) L = 3 mm (c) L = 0 mm

Fig. 4. The acoustic intensity curves.

4. Experimental results

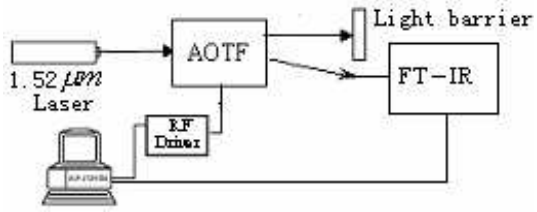

Fig. 5. The setup of experiment for diffraction efficiency of AOTF.

Based on the analysis, three AOTFs with different transducers (L = 6 mm, 3 mm, 0 mm) were made，and the experiment setup was designed to measure AOTF and get the spectrums of the diffracted light through FT-IR. The optical source is He-Nelaser (1.52 μm). Through these spectrums, we can get the curves of diffraction efficiency of AOTF with different transducers shown in Fig. 6. And we know the sidelobe of transducer whose geometry is triangle (L = 0 mm) is less.

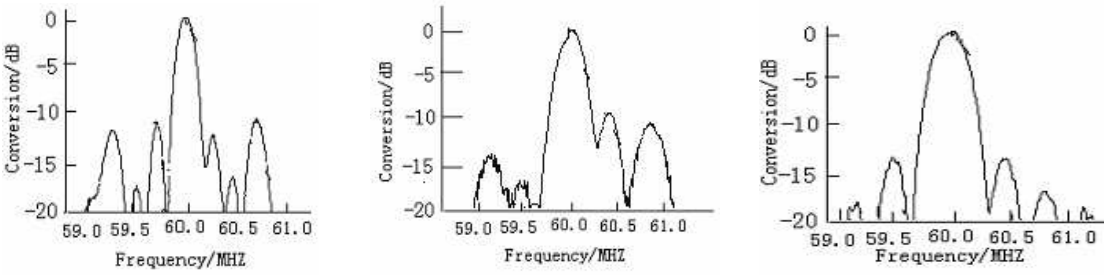

(a) L = 6 mm (b) L = 3 mm (c) L = 0 mm

Fig. 6. The plot of diffraction efficiency of AOTF.

The results show the sidelobe of transducer whose geometry is triangle(L = 0 mm) is less than the other by 4%，as shown in Table 1.

Table 1. Sidelobe corresponding to the shape of transducer.

Transducer	Sidelobe %
L = 6 mm	45.1
L = 0 mm	41.1

5. Optimum transducer geometry

Proceeding from the discussed results, it is clear that the filter transmission function depend on the acoustic distribution form. It is desirable for experimental acousto-optical devices to have rectangular profile bandwidth and lower sidelobe. To obtain such a bandwidth it is natural to feed acoustic intensity distribution with a sinc(x) envelope: the Fourier spectrum of this function being rectangular. So the transducer geometry is designed and its acoustic intensity distribution is shown in Fig. 7(a). Clearly the sidelobe is less than Fig. 4 (L = 0 mm), and its first order maximum is not so acute. But it is difficult to make this transducer, another transducer geometry is designed as shown in

Fig. 7(b) and its acoustic intensity distribution is also calculated. Its acoustic intensity distribution form is close to sinc(x) envelope. So we believe its results will be better than others. The experiment about it will be given in following papers.

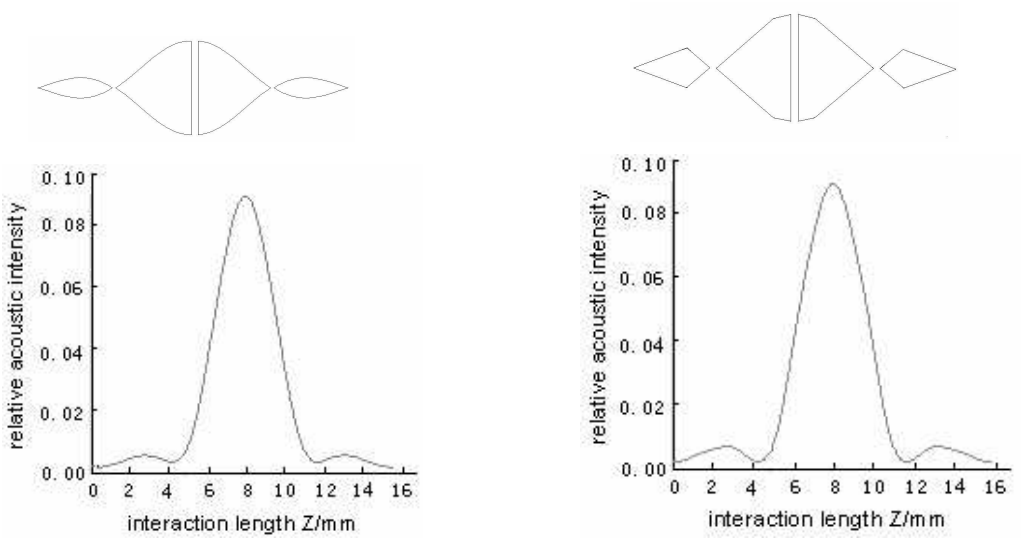

(a) sinc(x) (b) close to sinc(x)

Fig. 7. The acoustic intensity curves.

6. Conclusion

In this paper, the acoustic intensity of different transducer geometries of AOTF were calculated in the near-infrared spectral monitoring system and the acoustic intensity curves were drawn. The results show that the change of transducer geometry lead to the change of the acoustic intensity, the sidelobe was suppressed and the spectral purity can be improved. Based on this, we present another transducer geometry to design AOTF, and its results are analyzed and discussed.

References

[1] D. A. Smith, J. J. Johnson, B. L. Heffner and et al. Two stages integrated optic acoustically tunable optical filter with enhanced sidelobe suppression. Electron Lett. **25**, 398 (1989).
[2] H. Herrmann, P. Muller-Reich, V. Reimann, R. Ricken and et al. Integrated optical, TE- and TM-pass acoustically tunable, double-stage wavelength filter in $LiNbO_3$. Electron. Lett. **28**, 642 (1992).
[3] H. Herrmann, St. Schmid. Integrated acousto-optical mode converters with weighted coupling using surface acoustic wave directional couplers. Electron Lett. **28**, 979 (1992).
[4] D. A. Smith, J. J. Johnson. Sidelobe suppression in an acousto-optic filter with raised-cosine interaction strength. Appl. Phys. Lett. **61**, 1025 (1992).
[5] V. Parygin, A. Vershoubskiy, E. Filatova. Improvement of the acousto-optic cell function by piezotransducer sectioning, Journal of Modern Optics **47**(9), 1501 (2000).
[6] H. Herrmann, K. Schafer, W. Sohler. Polarization independent, integrated optical, acoustically tunable wavelength filters/switches with tapered acoustical directional coupler, IEEE, Photon Technol. Lett. 6(11), 1335 (1994).
[7] Arjun Kar-Roy, Chen S. Tsai. Ultra low sidelobe-level integrated acousto-optic tunable filters using tapered-gap surface acoustic wave directional couplers. J. Lightwave Technol. **12**(6), 977 (1994).
[8] Du Gonghuan. The basics of acoustic. Shanghai scientific & technical publishers 106 (1981).
[9] B. A. Auld. Acoustic Fields and Waves in Solids (vol.1), John Wiley & Sons, Inc. 214 (1973).